Korean J. Chem. Eng., **26**(2), 534-541 (2009)

Application of gain scheduling for modeling the nonlinear dynamic characteristics of NO_x emissions from utility boilers

Liang Kong*, Yanjun Ding*,†, Yi Zhang, Lichuan Yuan*, and Zhansong Wu***

*Department of Thermal Engineering, Tsinghua University, Beijing 100-084, China
**School of Energy and Power Engineering, Dalian University of Technology, Dalian 116-024, China
(*Received 17 July 2008 • accepted 15 October 2008*)

Abstract−A hierarchical gain scheduling (HGS) approach is proposed to model the nonlinear dynamics of NO_x emissions of a utility boiler. At the lower level of HGS, a nonlinear static model is used to schedule the static parameters of local linear dynamic models (LDMs), such as static gains and static operating conditions. According to upper level scheduling variables, a multi-model method is used to calculate the predictive output based on lower-level LDMs. Both static and dynamic experiments are carried out at a 360 MW pulverized coal-fired boiler. Based on these data, a nonlinear static model using artificial neural network (ANN) and a series of linear dynamic models are obtained. Then, the performance of the HGS model is compared to the common multi-model in predicting NO_x emissions, and experimental results indicate that the proposed HGS model is much better than the multi-model in predicting NO_x emissions in the dynamic process.

Key words: Utility Boiler, Gain Scheduling, NO_x Emissions, Nonlinear Dynamic Model

INTRODUCTION

Static models and dynamic models are two common methods used in constructing models for the characteristics of NO_x emissions of utility boilers. Due to the complexity of formation mechanism of NO_x, neither static principle models nor dynamic principle models can be calculated accurately on-line. For this issue, experimental models are usually used in practice [1-5]. Static experiments take a long time, and the average value can reduce the error caused by the disturbances effectively, so the static models are usually reliable [1,4-7]. Taking account of the security of the units, step response is the common choice in dynamic experiments. Since dynamic processes cannot last for a long time and dynamic experiments are easily affected by disturbances, the dynamic characters are usually not accurate enough to achieve effective dynamic prediction [8,9].

Over the years, as indicated in the survey paper [10], gain scheduling has proven to be a popular approach for nonlinear control system design in a variety of application areas, such as flight control, automotive engine control and chemical process control [11]. The idea of the gain scheduling model is to design a family of linear dynamic models for several operating conditions and then schedule the models according to varying parameters, i.e., scheduling variables, which capture the system's nonlinear dynamics due to varying operation conditions [12,13]. This effectively relieves robustness requirements for a large range of operation points, so therefore better performance can be expected [12]. Multi-model [14-16], a widely used dynamic modeling method, calculates predictive outputs from a series of linear dynamic models (LDMs) through an interpolation rule. This method can be regarded as a type of gain scheduling model. However, as mentioned above, the inaccuracy of dynamic data will affect the performance of a single linear dynamic model, and the error finally infects the output of the whole multi-model. So the predictive result of a multi-model is often unacceptable.

Because the static model and the dynamic model are related, according to a given working condition, a nonlinear static model is used to schedule the static parameters of LDMs, such as static gains and static operating conditions. Then the potential output is predicted by multi-model method based on these LDMs. In this paper, this modeling method is termed hierarchical gain scheduling (HGS). Taking NO_x emissions for example, HGS makes use of a relatively accurate nonlinear static model to adjust static gains and operating conditions of the rough LDMs in real time. Experimental results demonstrated that HGS significantly outperforms the common multi-model method in predicting NO_x emissions.

MODELING PRINCIPLE OF HGS

1. Theory of Hierarchical Gain Scheduling

To ensure the accuracy of the dynamic model gained from linearization of the nonlinear system, the local linear dynamic model should only be used in the specific static operating condition [11]. But it is hard to depict the large-scale nonlinear dynamics with a number of linear models gained from respective static operating conditions. The idea of gain scheduling is to improve the accuracy of large-scale prediction by adjusting the local linear models through measuring scheduling variables in real time.

Gain scheduling in modeling is generally understood as the design of a specific gain scheduling method and its use in adjusting or scheduling the local linear models at typical static operating conditions. Then a large-scale accuracy prediction is realized. Designing this method involves the selection of scheduling variables and the determination of scheduling rules [17]. Scheduling variables are generally those measurable variables having most important impact

†To whom correspondence should be addressed.
E-mail: dyj@mail.tsinghua.edu.cn
‡This paper was presented at the 7th China-Korea Workshop on Clean Energy Technology held at Taiyuan, Shanxi, China, June 25-28, 2008.

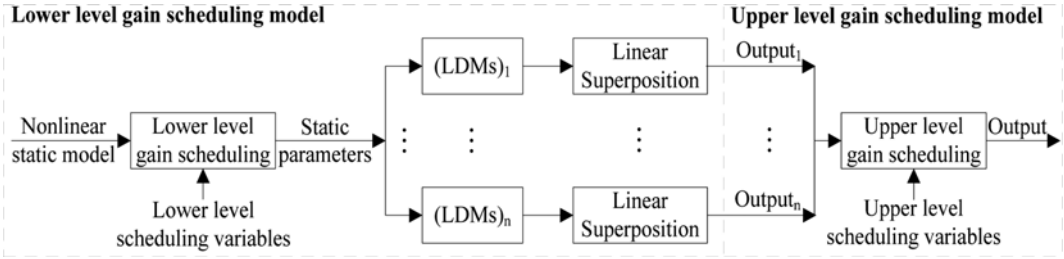

Fig. 1. The structure of HGS model.

on the dynamics of the objects. Taking NO_x emissions of utility boilers, for example, the load, air distribution and oxygen concentration of flue gas can be chosen as the scheduling variables. The scheduling rule determines which model is optimal for the current scheduling variables. It is generally divided into two categories: hard switch and soft switch. Hard switch directly chooses the local model whose operating condition is the most similar to the current operating condition, but this will lead to strong fluctuation of output. Soft switch is actually an application of interpolation method, which can be used for interpolating either the output values or the parameters of the models [13,18-20]. As soft switch offers smoother transitions for the output predictions, it is widely implemented.

The HGS model proposed in this paper improves the common scheduling rule. Fig. 1 shows the structure of the HGS model. According to lower level scheduling variables, a nonlinear static model is used to schedule the static parameters of local LDMs, such as static gains and static operating conditions. There are usually several groups of local LDMs. So each group provides a predictive output through linear superposition. The lower level which will be introduced in detail later is the core of HGS. Several predictive outputs are obtained with lower level gain scheduling model. According to upper level scheduling variables, final predictive output is gained by interpolation of these predictive outputs. A common linear interpolation method is used in this level. The combination of these two models leads to an HGS model.

2.Realization of HGS Model

In this section, realization of lower level of HGS is presented. Using static model to adjust linear dynamic models is inspired by the Hammerstein model structure. The Hammerstein model shown in Fig. 2 contains a static nonlinearity in series with a linear dynamic system. The nonlinear element precedes the linear block. Nonlinear static model with input u(k) is used to achieve immeasurable intermediate variable x(k), which acts as the input of linear dynamic model to predict the output y(k) [21]. Based on the Hammerstein model, a gain scheduling model can be constructed as follows: u(k) is chosen as the scheduling variable, x(k) adjusted by current u(k) is the static parameter of local LDMs, y(k) is acquired by linear superposition of adjusted LDMs.

To show the principle of using nonlinear static model to adjust the linear dynamic model, we assume that the nonlinear static model f_{ss} has been obtained from mechanism analysis or experimental data,

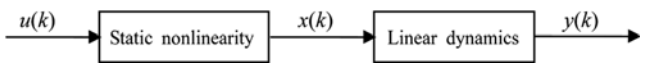

Fig. 2. The Hammerstein model structure.

and there is only one group of LDMs, which are $G_1(s)$, …$G_n(s)$.

2-1. Static Model

Nonlinear static model can be represented as

$$f_{ss}=f(MV_1, \ldots, MV_n, DV_1, \ldots DV_m), \tag{1}$$

where MVs (Manipulable Variables) and DVs (Disturbance Variables) are the inputs of this model.

2-2. Dynamic Model

Dynamic linear models of thermal objects with self-balancing ability are usually described as

$$G_i(s)=\frac{\Delta y_i}{\Delta MV_i}=\frac{b_1 s+g_i}{a_2 s^2+a_1 s+1}e^{-T_{di}s} \qquad i=1, 2, \ldots\ldots n, \tag{2}$$

Where $T_{di}=n_{di}T_s$, T_s is the sample interval [22]. Removing the delay temporarily, Eq. (2) can be transformed into the differential equation

$$a_2\frac{d^2\Delta y_i}{dt^2}+a_1\frac{d\Delta y_i}{dt}+\Delta y_i=b_1\frac{d\Delta MV_i}{dt}+g_i\Delta MV_i. \tag{3}$$

Substituting differentials in Eq. (3) with following differences

$$\frac{d^2\Delta y_i}{dt^2}=\frac{\Delta y_{i_k}-2\Delta y_{i_{k-1}}+\Delta y_{i_{k-2}}}{T_s^2}, \tag{4}$$

$$\frac{d\Delta y_i}{dt}=\frac{\Delta y_{i_k}-\Delta y_{i_{k-1}}}{T_s}, \tag{5}$$

$$\frac{d\Delta MV_i}{dt}=\frac{\Delta MV_{i_k}-\Delta MV_{i_{k-1}}}{T_s}, \tag{6}$$

and taking the delay into consideration, Eq. (2) can be converted into

$$\Delta y_{i_k}=\frac{2a_2+a_1T_s}{m}\Delta y_{i_{k-1}}-\frac{a_2}{m}\Delta y_{i_{k-2}}+\frac{b_1T_s+g_iT_s^2}{m}MV_{i_{k-n_i}}-\frac{b_1T_s}{m}MV_{i_{k-n_i-1}}-\frac{g_iT_s^2}{m}MV_{i_0}, \tag{7}$$

Where $m=a_1+a_2T_s+T_s^2$, $\Delta y_i=y_i-y_0$.

2-3. Combining Dynamic Model with Static Model

Set model inputs as $\mathbf{u}_k=[MV_1, \ldots MV_n, DV_1, \ldots DV_m]_k^T$. Describe static operating point as $(\mathbf{u}_0, y_0)$, which satisfies $y_0=f_{ss}(\mathbf{u}_0)$. And we assume that Eq. (1) is differentiable at $\mathbf{u}_k$. In the Hammerstein model, let $\mathbf{u}(k)=\mathbf{u}_k$, $\mathbf{x}(k)=[y_0, g_1, \ldots g_n]_k^T$. Where $y_0=f_{ss}(\mathbf{u}_k)$, and $g_i=(\partial f_{ss}/\partial MV_i)|_{\mathbf{u}=\mathbf{u}_k}$. Taking new y_0, g_i and MV_{i_0} into Eq. (7), a new dynamic model on the basis of gain scheduling is yielded.

Let MV_{i_0} equal to $MV_{i_{k-n_{di}}}$, Eq. (7) can be rewritten as

$$\Delta y_{i_k}=\frac{2a_2+a_1T_s}{m}\Delta y_{i_{k-1}}-\frac{a_2}{m}\Delta y_{i_{k-2}}+\frac{b_1T_s}{m}(MV_{i_{k-n_{di}}}-MV_{i_{k-n_{di}-1}}). \tag{8}$$

In this case, the calculation of g_i is avoided, and the predictive model is further simplified.

The above method can be regarded as an approximate continuous linearization procedure. Theoretically, if both the static model and dynamic model are accurate, the result is an accurate description of the nonlinear dynamic characteristics.

2-4. Output of Dynamic Prediction

The predictive output y_k is calculated by superposition with respect to a group of LDMs, i.e.,

$$y_k = y_0 + \sum_{i=1}^{n} \Delta y_{i_k}. \quad (9)$$

The above four steps realize the lower level gain scheduling model. If there are several groups of LDMs, several different y_ks are acquired from lower level model. Then, in terms of upper level gain scheduling model using a common linear interpolation method, the final predictive output y_k is obtained.

3. Simulation Example

Consider a single-input single-output (SISO) nonlinear system:

$$\frac{dy}{dt} + y = \frac{du}{dt} + u^2. \quad (10)$$

3-1. Static Model

Obviously, the static model is $y_{ss}=u^2$, and static gain is $g=(\partial y_{ss}/\partial u)=2u$.

3-2. Dynamic Model

Static operating point as (u_0, y_0) satisfies

$$y_0=u_0^2. \quad (11)$$

Eq. (10)-Eq. (11):

$$\frac{d(y-y_0)}{dt} + y - y_0 = \frac{d(u-u_0)}{dt} + u^2 - u_0^2. \quad (12)$$

Linearizing at u_0, i.e., taking $u^2 \approx u_0^2 + g(u_0)(u-u_0)$ into Eq. (12), we get the linear dynamic model

$$\frac{d(y-y_0)}{dt} + y - y_0 = \frac{d(u-u_0)}{dt} + g(u_0)(u-u_0). \quad (13)$$

Eq. (13) can be transformed into $G(s)=\frac{\Delta y(s)}{\Delta u(s)}=\frac{s+g(u_0)}{s+1}$.

Using difference instead of differential, Eq. (13) becomes

$$\Delta y_k = \frac{1}{T_s+1}[\Delta y_{k-1} + (1+g(u_0)T_s)u_k - u_{k-1} - g(u_0)T_s u_0]. \quad (14)$$

3-3. Combine Dynamic Model with Static Model

Always choose $u_0=u_k$, $y_0=y_{ss}(u_0)=u_k^2$, then Eq. (14) is reduced to

$$\Delta y_k = \frac{1}{T_s+1}[\Delta y_{k-1} + u_k - u_{k-1}]. \quad (15)$$

3-4. Output of Dynamic Prediction

Taking $\Delta y_k = y_k - y_0 = y_k - u_k^2$ and $\Delta y_{k-1} = y_{k-1} - y_0 = y_{k-1} - u_k^2$ into Eq. (15), the output of dynamic prediction is given by

$$y_k = \frac{1}{T_s+1}[y_{k-1} + T_s u_k^2 + u_k - u_{k-1}]. \quad (16)$$

3-5. Validation

Using forward difference instead of the differential in Eq. (10) directly, the result $y_k=1/(T_s+1)[y_{k-1}+T_s u_k^2+u_k-u_{k-1}]$ is the same as Eq. (16). Therefore, the correctness of the HGS model is validated.

3-6. Compared with the Common Multi-model Method

Let $\Delta y=y-y_0$ and $\Delta u=u-u_0$, then $G(s)=\frac{\Delta y(s)}{\Delta u(s)}=\frac{s+g(u_0)}{s+1}$.

Based on local linearization, we can obtain $G_1(s)=\frac{\Delta y(s)}{\Delta u(s)}=\frac{s}{s+1}$ at static operating point (0,0), and $G_2(s)=\frac{\Delta y(s)}{\Delta u(s)}=\frac{s+20}{s+1}$ at static operating point (10,100).

With current input, multi-model outputs are calculated by linear interpolation of the current outputs of $G_1(s)$ and $G_2(s)$.

The variation of input of simulation is shown in Fig. 3. The corresponding predictive results of both the multi-model and HGS model are displayed in Fig. 4, which indicates that the common multi-model method is only effective at the linearized operating point (u=10), and the HGS model can realize large-scale accurate prediction.

3-7. Conclusion

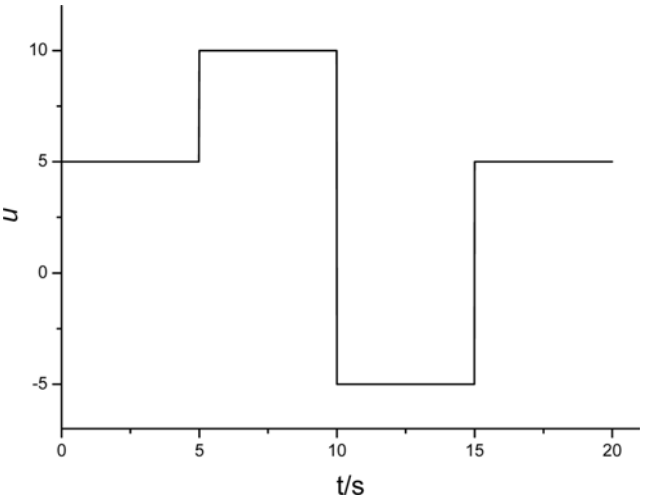

Fig. 3. Variation of input *u* in simulation.

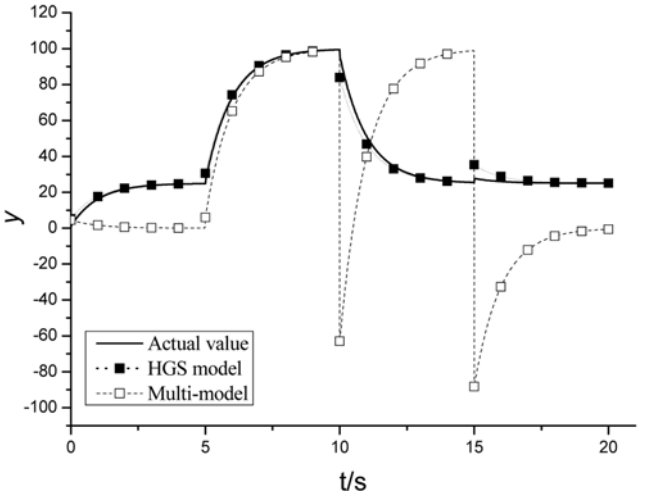

Fig. 4. Time response of output *y* in simulation.

Local dynamic models are gained from linearization of the nonlinear system, so the multi-model can only have good performance near linearized points. In contrast with the multi-model, the HGS model utilizes the information of the nonlinear static model to adjust the dynamic model. Hence, it has better capability in dynamic prediction.

It should be noted that for this SISO nonlinear system, if both static model y_{ss} and linear dynamic model G(s) are absolutely accurate, a precise description of nonlinear objects can be acquired by HGS model.

4. Experiments

Experiments are carried out at a 360 MW pulverized coal-fired boiler with W-type flame [23,24]. Fig. 5 is the sketch of the furnace structure; 36 direct burners are fixed at the forward arc and back arc in two lines and shoot down towards the center of the furnace bottom, flame flow upwards at the cold ash funnel, then W-type flame is formed. This structure can make the best use of the anthracite containing low volatility and high ash. A CEMS (continuous emission monitoring system) produced by TALROAD was installed between electrostatic precipitators and desulfurization tower to measure NO_x in real time.

Static experiments used the orthogonal experiment design method, while dynamic experiments used the step response method. Considering practical operating conditions, seven variables (primary air pressure, secondary air A damper position, secondary air B damper position, secondary air C damper position, upper tertiary air damper position, lower tertiary air damper position, O_2 concentration of flue gas) are chosen as MVs. As operation performances are different under different loads, three typical loads (100%, 85%, 70%) are chosen for experiments so as to cover normal operation.

RESTULTS AND DISCUSSION

1. Static Model

Orthogonal experiment design method including seven factors and three levels is applied in each typical load. And 107 groups of available experimental data are acquired. Because artificial neural networks (ANNs) have been applied to model nonlinear objects successfully in various fields of mathematics, engineering, medi-

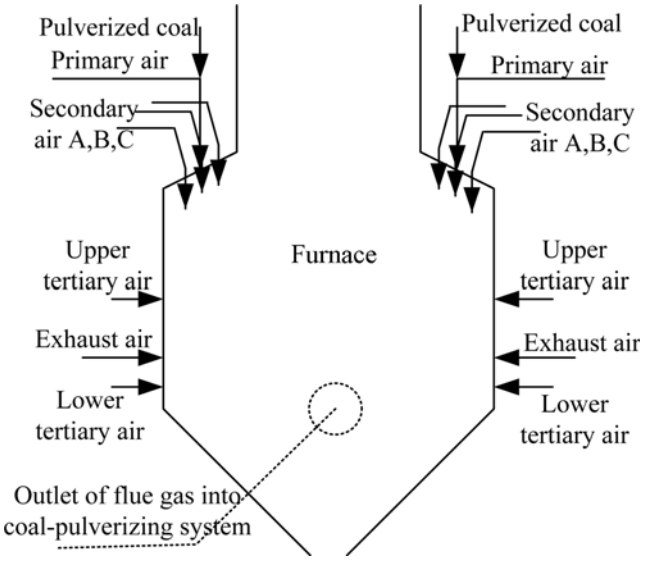

Fig. 5. Sketch of furnace structure of experimental boiler.

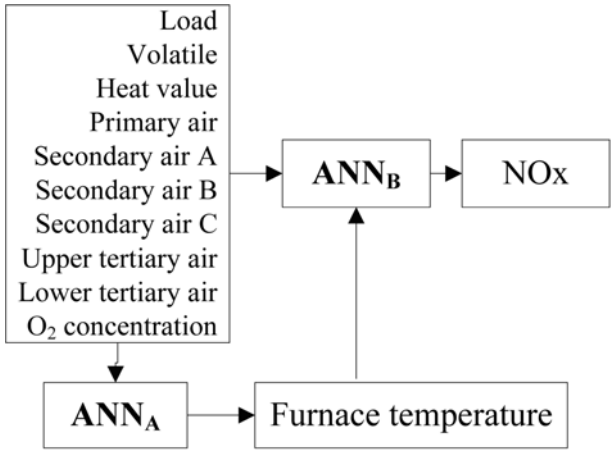

Fig. 6. Structure of static ANN model of NO_x emissions.

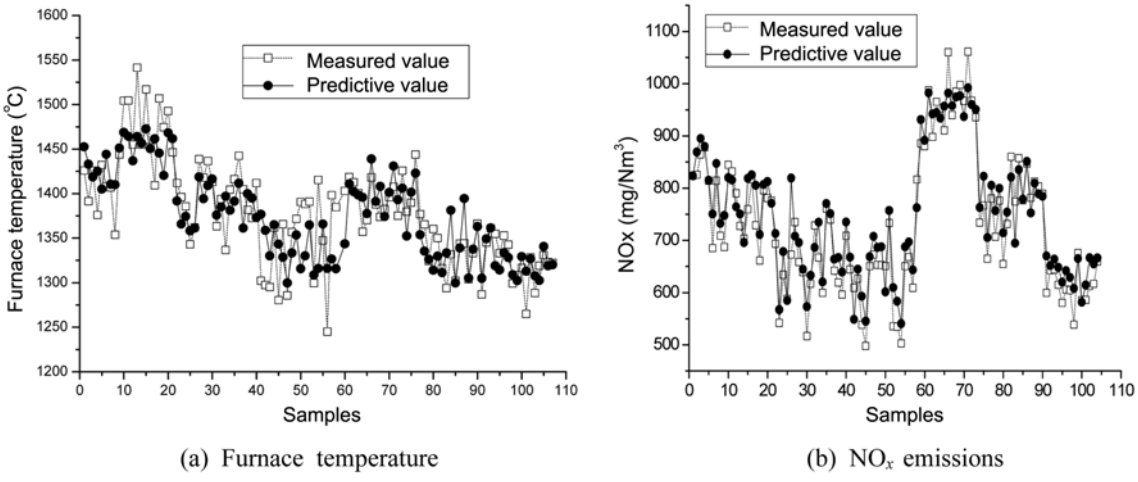

(a) Furnace temperature (b) NO_x emissions

Fig. 7. Modeling results of BP ANNs.

cine, economics and many others [25]. The static model of NO_x is built based on ANN, and the model structure is shown in Fig. 6. ANNs are all in a feedforward structure with training algorithm of back-propagation (BP), and a sigmoid function is chosen as the activation function to ensure continuity. Because furnace temperature is very important to NO_x emissions, ANN_A is used to predict furnace temperature at first.

Static predictive ANN models are

$$FT_{ss}=f_{ANN_A}(\mathbf{MV}, \mathbf{DV}) \tag{17}$$

and

$$NOx_{ss}=f_{ANN_B}(\mathbf{MV}, \mathbf{DV}, FT_{ss}), \tag{18}$$

where

MV=[primary air pressure, secondary air A damper position, secondary air B damper position, secondary air C damper position, upper tertiary air damper position, lower tertiary air damper position, O_2 concentration of flue gas]$^T_{ss}$;

DV=[Load, Coal volatile, Coal heat value]$^T_{ss}$.

Eq. (17) is the model of furnace temperature. The structure is 10-5-1 (10 input nodes, 5 hidden nodes and 1 output node). The modeling result of furnace temperature is displayed in Fig. 7(a), and the average relative error is 1.98%. Model of NO_x is shown in (18), the structure is 11-5-1, the modeling result is displayed in Fig. 7(b), and the average relative error is 4.72%. These static ANN models are effective and available.

2. Dynamic Model

According to the three typical loads, dynamic experiments are also divided into three groups. Then step responses for seven MVs are carried out in each load. Based on the responding curves, all the transfer functions can be approximately given by

$$G(S)=\frac{g}{1+T_pS}e^{-T_dS}. \tag{19}$$

In this paper, all the parameters are identified by least square method.

Using forward difference instead of differential in (19), difference form is given by

$$\Delta y_k=\frac{T_p}{T_p+T_s}\Delta y_{k-1}+\frac{gT_s}{T_p+T_s}(u_{k-n_d}-u_0), \tag{20}$$

where, $n_d=T_d/T_s$, T_s denotes the sample interval, which is 5 seconds. Taking the example of primary air pressure, the step-response curve and fitting curve are displayed in Fig. 8. All the parameters of the transfer functions are listed in Table 1.

3. HGS Model in Practical Application

Based on the static model and dynamic model, the calculation process of the HGS model is shown in Fig. 9. The initial condition must be a static operating condition, which is used to provide the initial values and compensate the error of the static model. Lower level scheduling variables consist of seven MVs and three DVs, while upper level scheduling variable is the load.

The first test was at 330 MW between high load and medium load. The boiler combustion was kept stable at first, and then only the seven MVs were adjusted to maintain the combustion stability. And this dynamic process lasted for 26 minutes. The measured values and predictive values are shown in Fig. 10. Using multi-model,

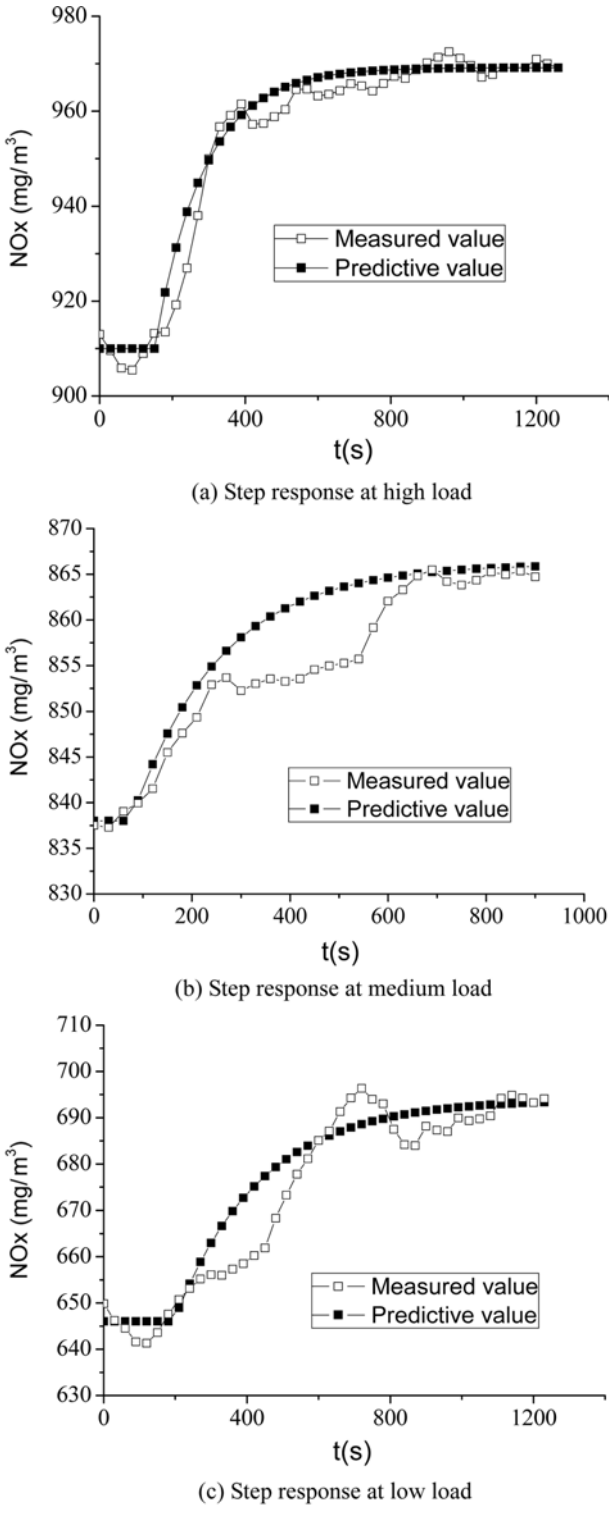

Fig. 8. Curves of step responses of primary air pressure and its fitting curves.

the average absolute error is 29 mg/Nm^3 and the average relative error is 3.55%; while the average absolute error is 20 mg/Nm^3 and the average relative error is 2.48% in the HGS model, which obviously improves the predictive accuracy.

The second test is at 280 MW between medium load and low load. The operator also kept combustion stable first, then only seven

Table 1. Dynamic model parameters of NO_x emissions of 7 MVs

Variable of step response	Load (MW)	Proportional coefficient (g)	Time constant (T_p)	Delay (T_d)	Initial NO_x (mg/Nm^3)	Step value
Primary air pressure	350	18.5	135	150	910	3.85-4.17
	300	17.6	180	165	836	3.64-3.8
	250	16	240	195	646	3.46-3.76
Secondary air A damper position	350	3.19	90	345	900	81-100
	300	3.8	90	210	790	40-58
	250	5	45	60	710	50-41
Secondary air B damper position	350	2.1	60	75	970	50-22
	300	4.6	180	120	840	15-3
	250	3.4	105	225	642	0-7
Secondary air C damper position	350	2.3	246	22	940	80-40
	300	3.3	135	195	784	60-80
	250	4.2	180	105	680	55-42
Upper tertiary air damper position	350	−2.1	195	270	980	57-85
	300	−1.78	270	225	800	40-20
	250	−1.35	240	165	658	50-20
Lower tertiary air damper position	350	−1.7	180	45	954	45-100
	300	−1.3	135	135	790	70-100
	250	−0.65	75	210	683	50-100
O_2 concentration of flue gas	350	50	195	120	940	1.5-2
	300	85	210	75	735	1.6-2.2
	250	95	255	135	622	2.4-2.95

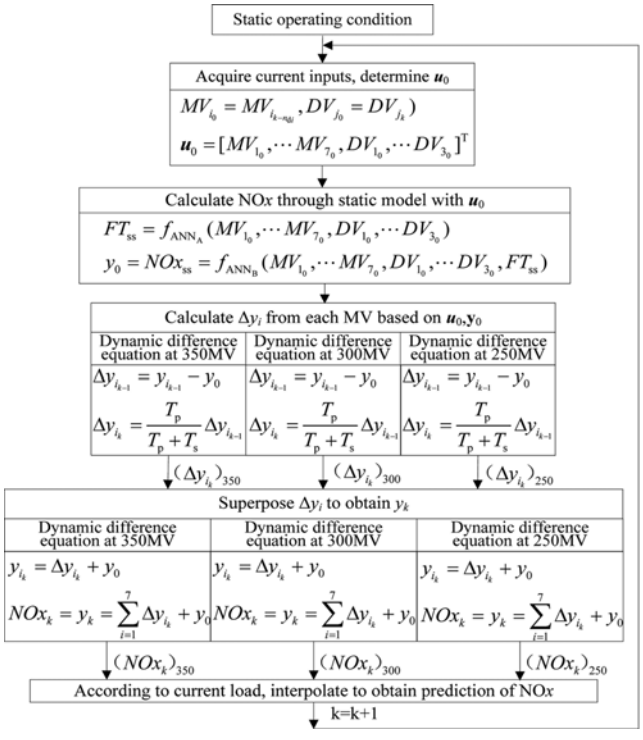

Fig. 9. Computational flowchart of HGS model.

MVs were used to adjust the combustion. This process lasted 42 minutes, and the results are displayed in Fig. 11. Using multi-model, the average absolute error is 30 mg/Nm^3 and the average relative error is 4.43%; while the average absolute error is 19 mg/Nm^3 and the average relative error is 2.75% in the HGS model, which greatly improves the predictive accuracy.

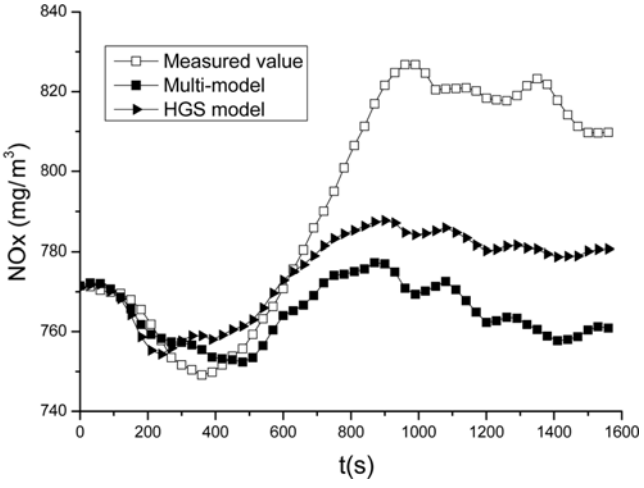

Fig. 10. Comparison of dynamic predictive results at 330 MW.

Moreover, Fig. 11 also shows that the HGS model not only can reduce the overall predictive error, but also track the intensive fluctuation in the first 1,000 seconds. O_2 concentration is closely related to NO_x emissions. The historic data shows that O_2 concentration changed from 2.2% to 1.2%, then went back to 2.4% in this process. In such an intensive fluctuation, constant linear dynamic models cannot work well, but the HGS model works well with continuous adjustments of the dynamic model.

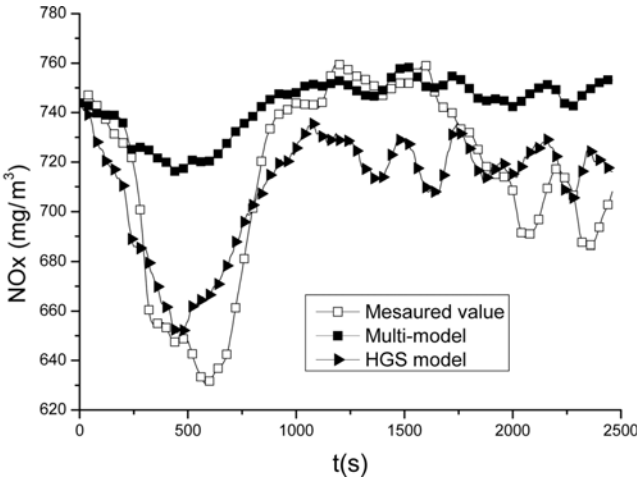

Fig. 11. Comparison of dynamic predictive results at 280 MW.

CONCLUSION

Step response is the prevailing practical choice for obtaining the dynamics of NO_x emissions of utility boilers. Considering the inaccuracy of the dynamic experimental data and the limitation of the applicable field of local LDMs, this paper proposes a nonlinear static model for adjusting the parameters of the linear dynamic model in real time. Therefore, an HGS nonlinear dynamic model of NO_x emissions is built.

Overall, the accuracy of the HGS model is validated theoretically by an SISO nonlinear system. After that, it's taken into practice for predicting NO_x emissions of a utility boiler, with steps as follows. First, data are obtained from field experiments; second, static and dynamic models are both constructed, finally, the HGS model is applied to predict NO_x emissions at two different loads. Hence, the prominent advantages of the HGS model over the common multi-model are evidently shown through both theoretic and practical applications.

NOMENCLATURE

a_1, a_2, b_1 : parameters in transfer function
ANN : artificial neural network
BP : back propagation
CEMS : continuous emission monitoring system
DV : disturbance variable
FT : furnace temperature [°C]
g : gain
G(s) : transfer function
HGS : hierarchical gain scheduling
k : discrete time
LDM : linear dynamic model
m : number of disturbance variables
MV : manipulable variable
n : number of manipulable variables
n_d : discrete delay time
NO_x : nitrogen oxides [mg/Nm^3]
s : complex argument
SISO : single-input single-output
T_d : delay time [s]
T_p : time constant [s]
T_s : sampling interval [s]
u : input
u : inputs in matrix
u_0 : initial static input
$\mathbf{u}_0$: initial static inputs in matrix
x : intermediate variable
y : output
y_0 : initial static output

Greek Letters
Δ : difference operator

Subscripts
0 : initial steady state
i : the i^{th} MV parameter
j : the j^{th} DV parameter
k : discrete time
ss : steady state

Superscripts
T : transpose

REFERENCES

1. Y. Zhang, Y. J. Ding, Z. S. Wu, L. Kong and T. Chou, *Korean J. Chem. Eng.*, **24**, 1118 (2007).
2. S. P. Visona and B. R Stanmore, *Chem. Eng. Sci.*, **53**, 2013 (1998).
3. C. F. M. Coimbra, J. L. T. Azevedo and M. G. Carvalho, *Fuel*, **73**, 1128 (1994).
4. H. Zhou, K. F. Cen and J. R. Fan, *Energy*, **29**, 167 (2004).
5. H. Zhou, K. F. Cen and J. B. Mao, *Fuel*, **80**, 2163 (2001).
6. A. J. Christopher and L. Roger, *Proceedings of int'l joint power generation conference*, Baltimore (1998).
7. R. C. Booth and W. B. Roland, *Proceedings of dynamic modeling control applications for industry workshop*, Vancouver (1998).
8. A. Laungphairojana, *Boiler operation optimization for air pollution control*, Vanderbilt Univ. Press (2003).
9. S. Piche, B. Sayyar-Rodsari, D. Johnson and M. Gerules, *Control Systems Magazine*, **20**, 53 (2000).
10. W. J. Rugh and J. S. Shamma. *Automatica*, **36**, 1401 (2000).
11. K. J. Astrom and B. Wittenamrk, *Adaptive control*, Beijing, Science Press (2003).
12. P. C. Chen and J. S. Shamma, *Journal of Process Control*, **14**, 263 (2004).
13. Z. Y. Huang, D. H. Li, X. Z. Jiang and L. M. Sun, *Proceedings of the CSEE*, **23**, 191 (2003).
14. V. Petridis and A. Kehagias, *Automatica*, **34**, 469 (1998).
15. L. Chen and K. S. Narendra, *Automatica*, **37**, 1245 (2001).
16. Y. Fu and T. Chai, *Automatica*, **43**, 1101 (2007).
17. J. R. Wilson and S. S. Jeff, *Automatica*, **36**, 1401 (2000).
18. F. C. Eduardo and A. O.Vilma, *Automatica*, **38**, 1247 (2002).
19. D. A. Lawrence, *Automatica*, **37**, 1041 (2001).
20. J. D. Francis, S. K. Harpreet and S. S. James, *Chem. Eng. Sci.*, **53**, 2675 (1998).
21. H. Al-Duwaish and W. Naeem, *Proceedings of the 2001 IEEE inter-*

national conference on control applications, Mexico City (2001).
22. A. T. Johjns and D. F. Warne, *Thermal power plant simulation and control*, London, The Institution of Electrical Engineers (2003).
23. L. L. Fang and Z. Y. Gao, *Proceedings of the CSEE*, **23**, 211 (2003).
24. D. H. Chung, J. B. Yang, D. S. Noh and W. B. Kim, *Korean J. Chem. Eng.*, **16**, 489 (1999).
25. S. A. Kalogirou, *Prog. Energy Combust. Sci.*, **29**, 515 (2003).